

Essentially entangled component of multipartite mixed quantum states, its properties, and an efficient algorithm for its extraction

V. M. Akulin,^{1,2} G. A. Kabatiansky,^{2,3} and A. Mandilara⁴

¹Laboratoire Aimé Cotton, CNRS (UPR 3321), Bâtiment 505, 91405 Orsay Cedex, France

²Institute for Information Transmission Problems of the Russian Academy of Science, Bolshoy Karetny per. 19, Moscow 127994, Russia

³Laboratoire J.-V. Poncelet CNRS (UMI 2615), Bolshoi Vlassievsky per. 11, Moscow 119002, Russia

⁴Department of Physics, School of Science and Technology, Nazarbayev University, 53, Kabanbay batyr Av., Astana, 010000, Republic of Kazakhstan

(Received 17 June 2015; published 20 October 2015)

Using geometric means, we first consider a density matrix decomposition of a multipartite quantum system of a finite dimension into two density matrices: a separable one, also known as the best separable approximation, and an essentially entangled one, which contains no product state components. We show that this convex decomposition can be achieved in practice with the help of a linear programming algorithm that scales in the general case polynomially with the system dimension. We illustrate the algorithm implementation with an example of a composite system of dimension 12 that undergoes a loss of coherence due to classical noise and we trace the time evolution of its essentially entangled component. We suggest a “geometric” description of entanglement dynamics and demonstrate how it explains the well-known phenomena of sudden death and revival of multipartite entanglements. For a statistical weight loss of the essentially entangled component with time, its average entanglement content is not affected by the coherence loss.

DOI: [10.1103/PhysRevA.92.042322](https://doi.org/10.1103/PhysRevA.92.042322)

PACS number(s): 03.67.Mn, 03.65.Ud, 03.67.Bg

I. INTRODUCTION

Although quantum entanglement is a concept that has attracted considerable attention of physicists working in various fields [1], there are, however, further research opportunities to develop a more complete understanding [2]. One of the main open problems is the efficient detection and characterization of a multipartite entanglement of density matrices representing open quantum systems undergoing nonunitary evolution [3].

All experimentally addressable information regarding a quantum physical system is contained in its density matrix $\hat{\rho}$. We focus on a multipartite quantum system, which comprises a finite number $K < \infty$ of parts \mathcal{N}_k numerated by index $k = 1, \dots, K$, each represented in the Hilbert space of a finite dimensionality N_k , where $\prod_{k=1}^K N_k = N$ is the dimensionality of the Hilbert space of the entire system. This system-assembly of parts, is not entangled (or separable) if and only if its density matrix can be cast into a statistical sum,

$$\hat{\rho} = \sum_{i=1}^M a_i \prod_{\otimes k=1}^K |\alpha_i^k\rangle\langle\alpha_i^k|, \quad (1)$$

where ($a_i > 0$, $\sum_{i=1}^M a_i = 1$) of M various ($i = 1, \dots, M$) direct products $\prod_{\otimes k=1}^K |\alpha_i^k\rangle\langle\alpha_i^k|$ of the density matrices $|\alpha_i^k\rangle\langle\alpha_i^k|$ of pure states $|\alpha_i^k\rangle$ of each part. A state for which the equality condition, Eq. (1), is not possible is called entangled (or inseparable), and such a state cannot be comprised by statistically independent elements.

Many approaches [2] have been developed aiming to answer the question of whether or not a density matrix is separable. Currently, there are no exact analytical methods applicable to the multipartite problem, and we do not believe in the existence of an exact analytical solution. An algorithmic solution to the “decision” problem [4] associated with separability has been proven to be a NP-hard problem [5], but valuable

progress has been made (mainly on the biseparability problem) in approaches [6–11], where semidefinite programming is merged with analytic criteria [12].

In this work we provide a geometric point of view on the problem of inseparability that suggests there is an efficient solution based on linear programming. By using simple geometric arguments, we conjecture an algorithm that results in a unique decomposition of the density matrix as

$$\hat{\rho} = (1 - B)\hat{\rho}_{\text{sep}} + B\hat{\rho}_{\text{ent}}, \quad (2)$$

where $\hat{\rho}_{\text{sep}}$ is the *separable component*, $\hat{\rho}_{\text{ent}}$ is the *essentially entangled* part that cannot have any separable states as components, while B is a positive number in the range $[0, 1]$. Obviously, the decomposition, Eq. (2), implies that the state $\hat{\rho}$ is separable in all K parts only for $B = 0$.

The decomposition in Eq. (2) was initially introduced in [13] without using a geometric picture. The component $(1 - B)\hat{\rho}_{\text{sep}}$ is widely known as *the best separable approximation* of the density matrix $\hat{\rho}$. In that same seminal work, the uniqueness of the decomposition was proven for the multipartite case and a strict upper bound on the rank of the component $\hat{\rho}_{\text{ent}}$ for the biseparable case. In this work we generalize the latter to the multipartite case, proving that the rank of $\hat{\rho}_{\text{ent}}$ is upper bounded by a number related to the dimensions of the total system and those of the subelements.

On a practical level, we show that the linear programming algorithm combined with a simple optimization technique allows one to efficiently find the decomposition of a generic density matrix,

$$\hat{\rho} = \sum_{i=1}^M a_i \underbrace{\prod_{\otimes k=1}^K |\alpha_i^k\rangle\langle\alpha_i^k|}_{\text{product states}} + \sum_{i=1}^m b_i \underbrace{|\beta_i\rangle\langle\beta_i|}_{\text{entangled states}}, \quad (3)$$

with the coefficients constrained by the requirements

$$a_i > 0, \quad b_i \geq 0, \quad \sum_{i=1}^M a_i + \sum_{i=1}^m b_i = 1, \quad (4)$$

$$\text{and } \sum_{i=1}^m b_i \rightarrow \min. \quad (5)$$

When this limit is reached, the decomposition in Eq. (3) yields Eq. (2), with $B = (\sum_{i=1}^m b_i)_{\min}$:

$$\hat{\rho}_{\text{sep}} = \sum_{i=1}^M \frac{a_i}{1-B} \underbrace{\prod_{k=1}^K |\alpha_i^k\rangle\langle\alpha_i^k|}_{\text{product states}} \quad (6)$$

and

$$\hat{\rho}_{\text{ent}} = \sum_{i=1}^m \frac{b_i}{B} \underbrace{|\beta_i\rangle\langle\beta_i|}_{\text{entangled states}}. \quad (7)$$

It is generally known that the linear programming method scales polynomially with the dimension of the vector space where it is applied. Using $M + m \leq N^2$ in Eq. (3), where N is the dimension of quantum assembly, we show that the proposed algorithm yielding the decomposition Eq. (3) scales as $(2N^4)^3$.

In Sec. II we introduce the idea of the decomposition of Eq. (2) and illustrate its uniqueness with a simple geometric picture generalizing the Bloch vector representation of a two-level system. This geometric picture helps to analyze some properties of $\hat{\rho}_{\text{ent}}$ and we conclude this section with a theorem setting an upper limit on its rank. In Sec. III we present a version of an efficient linear programming algorithm allowing one to explicitly find the decomposition of Eqs. (3)–(5) for a generic density matrix. In Sec. IV we suggest methods for characterizing the entanglement of the component $\hat{\rho}_{\text{ent}}$ which naturally reflects the entanglement properties of $\hat{\rho}$. In Sec. V we present a physical example which demonstrates the implementation of the technique introduced in previous sections and connect it with known notions in open quantum system dynamics. We conclude with the discussion in Sec. VI.

II. THE GEOMETRIC METHOD OF DECOMPOSITION AND PROPERTIES OF THE ESSENTIALLY ENTANGLED PART

All possible density matrices of a quantum system with a Hilbert space of dimension N comprise a convex set of positive Hermitian matrices of unit trace. This set can be viewed as a manifold in the vector space of Hermitian matrices endowed with a metric given by the Hilbert-Schmidt inner product $\text{tr}[\hat{\rho}_i, \hat{\rho}_j]$. The requirement of the unit trace in this representation means that the inner product of a vector representing a density matrix and a vector representing the unit matrix equals unity. In this paper, this manifold is called a ‘‘Liouville vector space.’’ Furthermore, the density matrix of a pure state has rank 1, which implies that the length of the vector corresponding to a pure state is equal to unity. The density matrix manifold is therefore a convex hull with unit-length vectors having a unit projection on the unity matrix.

A natural basis for such a vector space exists, spanned by the N^2 properly normalized generators \hat{g}_i^N of the unitary group $\text{SU}(N)$, including the unity $\hat{I} = \sqrt{N}\hat{g}_0^N$. This basis allows one to cast a $N \times N$ density matrix of a quantum system as $\hat{\rho} = \sum_{i=0}^{N^2-1} \hat{g}_i^N r_i$, with $r_i = \text{Tr}[\hat{g}_i^N, \hat{\rho}]$ as the N^2 real vector components. This geometric picture is a direct analogy to the Bloch vector for two-level systems.

The pure quantum states, represented by positive Hermitian density matrices of rank 1 and unit trace, lie at the surface of the unit hypersphere, since $\text{Tr}[\hat{\rho}^2] = \sum_{i=0}^{N^2-1} r_i^2 = 1$ is implicit. For $N > 2$, in contrast to the Bloch vector of two-dimensional pure quantum states, these states do not cover the complete surface of the unit hypersphere but are confined on a manifold of lower dimensionality. This is a consequence of the fact that for $N > 2$, the condition $\text{Tr}[\hat{\rho}^2] = \sum_{i=0}^{N^2-1} r_i^2 = 1$, together with the condition of the unit trace, does not guarantee that the density matrix is of rank 1 and an extra number of additional conditions needs to be imposed. These additional constraints can be understood when the characteristic polynomial $\text{Det}[\lambda - \hat{\rho}] = \lambda^N + c_1(\{r_i\})\lambda^{N-1} + c_2(\{r_i\})\lambda^{N-2} + \dots + c_N(\{r_i\})$ of a pure state is considered. The unit trace condition sets $c_1(\{r_i\}) \equiv -1$, while the rank-1 requirement implies the constraints $c_m(\{r_i\}) = 0$ for $m = 2, \dots, N$. The set of these N conditions on the N^2 components of the vector constrains the vector representing a pure state to lie on a restricted manifold of lower dimension $(N^2 - N)$ at the surface of the unit hypersphere. As a consequence, the density matrices for quantum systems of dimension $N > 2$ do not ‘‘fill’’ the whole inner part of the unit hypersphere, but they are lying inside an $(N^2 - 2)$ -dimensional body formed as a convex hull of the pure states of the $(N^2 - N)$ -dimensional manifold. This convex hull plays the role of the Bloch ball for higher dimensions of the Hilbert space and has been studied in [14] for the case of three-dimensional systems and in [15] for any N . The convex hull is touching the unit hypersphere only for the pure states, while its outer hyper-surface, which we denote by S_{CH} , is naturally the border between positive and nonpositive Hermitian matrices of unit trace. Therefore S_{CH} consists only of the degenerate density matrices which have at least one zero eigenvalue. In Fig. 1(b) we symbolically illustrate the convex hull of pure states such that all density matrices are inside this body.

The situation is similar for the convex hull formed exclusively by the pure product states. The product states, however, form a manifold of measure zero in the set of all states, and therefore the convex hull of pure product states is located inside the convex hull of all pure states—except for the points at the unit hypersphere corresponding to the pure product states. At the same time, the outer surface of this convex hull does not separate positive from negative matrices and consequently must not exclusively contain degenerate matrices. Figure 1(a) illustrates the situation symbolically by showing pure product states as points on the spherical surface and the convex hull of these points by a polytope inside the sphere. The states on the surface and inside the polytope are separable.

Figure 1(c) shows inseparable states as points inside the convex hull body of pure states but outside the polytope of the product states. Figures 1(e)–1(f) further illustrate the geometric meaning of Eq. (2), i.e., each mixed state can be represented as a sum of a separable state on the surface of

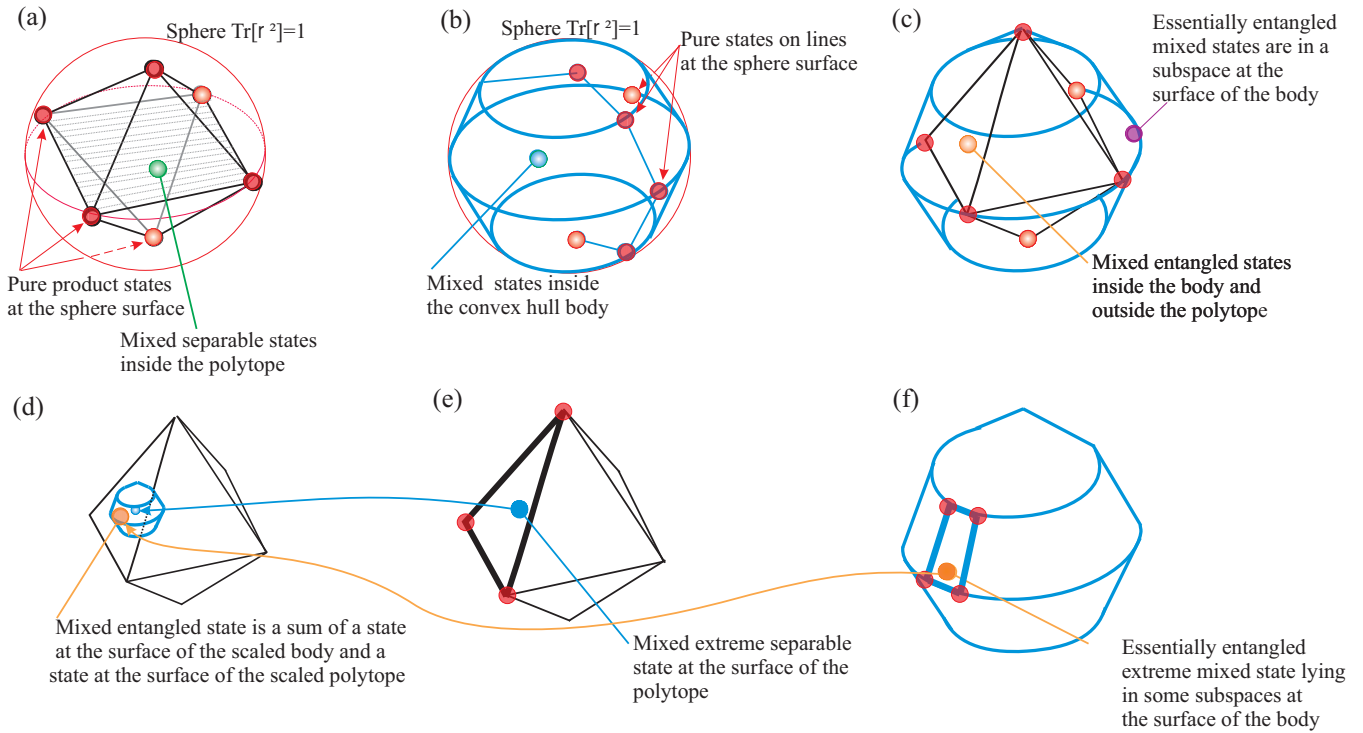


FIG. 1. (Color online) A symbolic illustration of the geometric structure of density matrices and of the decomposition Eq. (2).

the polytope within a scaled sphere of radius $1 - B$ and an essentially entangled state on the surface of the body within a scaled sphere of radius B . This geometric picture demonstrates the uniqueness of the decomposition in Eq. (2), a property that has been formally proven in Ref. [13].

It can be shown that the essentially entangled component $\hat{\rho}_{\text{ent}}$ is a density matrix of rank d_E strictly less than the dimension N of the Hilbert space of the entire system. The essentially entangled component belongs to the outer hypersurface S_{CH} of the convex hull of all states. Not every state on S_{CH} is an essentially entangled component; only the ones which do not contain the separable part [Fig. 1(c)]. In addition, the eigenvectors of $\hat{\rho}_{\text{ent}}$, $|\psi_l\rangle$ of $\hat{\rho}_{\text{ent}}$ with $l = 1, \dots, d_E$, are necessarily K -entangled pure states in the sense that these cannot be written as direct products of K pure states corresponding to the K subsystems. Therefore we can label pure states which are direct products of K pure states of K subsystems as K -product states.

Let us consider the Hilbert space H_E of dimension d_E associated with the eigenvectors $|\psi_l\rangle$ of $\hat{\rho}_{\text{ent}}$. Each state $|\bar{\psi}\rangle$ belonging to the Hilbert space H_E is a linear combination of the eigenvectors $|\psi_l\rangle$:

$$|\bar{\psi}\rangle = \sum_{l=1}^{d_E} \lambda_l |\psi_l\rangle. \quad (8)$$

The vector $|\bar{\psi}\rangle$ can be seen as a result of the action of an element \hat{U}_E of the unitary group $\text{SU}(d_E)$ associated with the Hilbert subspace H_E on one of the eigenvectors:

$$|\bar{\psi}\rangle = \hat{U}_E |\psi_1\rangle. \quad (9)$$

The convex hull of the states $|\bar{\psi}\rangle$ of the subspace naturally contain $\hat{\rho}_{\text{ent}}$. The condition that $\hat{\rho}_{\text{ent}}$ does not have any separable

components, $|\psi_{\text{prod}}\rangle\langle\psi_{\text{prod}}|$, implies that the convex hull does not contain a product state $|\psi_{\text{prod}}\rangle\langle\psi_{\text{prod}}|$; this is possible only if the Hilbert space H_E does not contain $|\psi_{\text{prod}}\rangle$. We call a Hilbert subspace with such a property an *essentially entangled subspace* of dimension d_E , and in what follows, with the help of this necessary condition, we find an upper bound on d_E .

Theorem II.1. The maximum rank $d_{E \text{ max}}$ of an essentially entangled component $\hat{\rho}_{\text{ent}}$ for a system of dimension N comprised by K subsystems, each of them of dimension N_k , is $N - \sum_{k=1}^K N_k + K - 1$.

Proof. Let us assume that the essentially entangled component $\hat{\rho}_{\text{ent}}$ is a density matrix of rank d_E and the subspace H_E is spanned by its K -entangled eigenvectors $\{|\psi_1\rangle, |\psi_2\rangle, \dots, |\psi_{d_E}\rangle\}$. Let us also consider the orthogonal complement of the subspace H_E , H_E^\perp of dimension $N - d_E$ and arbitrarily select a set of mutually orthogonal vectors $\{|\chi_1\rangle, |\chi_2\rangle, \dots, |\chi_{N-d_E}\rangle\}$ spanning H_E^\perp .

The subspace H_E is not essentially entangled if there is at least one product state $|\psi_{\text{prod}}\rangle$ that can be expressed as in Eq. (8),

$$|\psi_{\text{prod}}\rangle = \sum_{l=1}^{d_E} \lambda_l |\psi_l\rangle, \quad (10)$$

where λ 's are complex numbers. Equation (10) implies that $|\psi_{\text{prod}}\rangle$ must be orthogonal to every element $\{|\chi_i\rangle\}$, with $i = 1, \dots, N - d_E$, of the chosen basis in H_E^\perp :

$$\langle\psi_{\text{prod}}|\chi_{i=1, \dots, N-d_E}\rangle = 0. \quad (11)$$

The maximum number of such conditions is equal to the number of parameters defining a product state, which for a K -product state amounts to $\sum_{k=1}^K N_k - K$. Therefore the

maximum rank of an essentially K -entangled density matrix cannot be equal or exceed $\sum_{k=1}^K N_k - K$.

The maximum rank is smaller when we refer to an essentially entangled component which does not contain any biseparable state (not only K product). In this case, one has to identify the bipartition of the system that yields the maximum number of parameters characterizing the product state in order to estimate the maximum rank. In the Appendix we provide a more detailed proof of this theorem.

In the case of a mixed state of a system of two qubits, the essentially entangled subspace is of dimension one, implying that the essentially entangled component can only be a pure entangled state. This result is in agreement with the bipartite case treated in [13], while the derived theorem generalizes the outcomes obtained in that work to the multipartite case. The example studied in Sec. V gives some preliminary evidence that $\widehat{\rho}_{\text{ent}}$ stays very near to pure states ($\text{Tr}[\widehat{\rho}_{\text{ent}}^2] \approx 1$), even though $d_{E_{\text{max}}} \rightarrow N$ for $N \gg 1$.

III. THE LINEAR PROGRAMMING ITERATION ALGORITHM THAT YIELDS THE ESSENTIALLY ENTANGLED COMPONENT OF A DENSITY MATRIX

In principle, one can numerically identify the essentially entangled component of an arbitrary density matrix by straightforwardly applying the linear programming algorithm to the convex hull of general pure states and the polytope of pure separable quantum states. The main obstacle of this method is the high dimensionality of the corresponding Liouville vector space, making such a direct approach intractable within any approximation. Taking as an example the simplest multipartite system consisting of three qubits, where the dimensionality (N^2) of the density matrix space is 64, even for the rather low-accuracy approximation attributing just 10 points per dimension, one encounters a polytope of over 10^{64} vertices.

Therefore this paper suggests a method to critically decrease the number of the vertices that enter as samples in the algorithm and, consequently, substantially decrease the computational complexity of the procedure. We first notice that the solution of the problem and, in general, any convex decomposition of the form Eq. (3), allows for at most N^2 nonzero coefficients a_i and b_i . This observation can be formally justified by a theorem of Carathéodory as mentioned in [8]. In the limit $B = (\sum_{i=1}^m b_i)_{\text{min}}$, the pure states are the vertices associated with the corners of the facets corresponding to the solution, as illustrated in Figs. 1(e)–1(f), while the other vertices can be discarded.

Therefore, as a first step we may randomly take N^4 product states, N^4 general states, and, in order to ensure the algorithmic stability, complement this set by the N^2 eigenvectors of the given density matrix. We then find the solution of the linear programming problem, typically having complexity $\sim (2N^4)^3$, and thereby identify at most $N^2 - J$ product states and J general states with nonzero coefficients a_i and b_i , respectively. The linear constraint imposed on the algorithm is the minimization of $\sum_{i=1}^m b_i$, and the solution provided is a “local” minimum for the given set of vectors fed to the algorithm. Our aim is to find the global minimum value of $\sum_{i=1}^m b_i$ that is equal to B by devising an iterative optimization loop.

For the second and subsequent steps, we apply to each of the product states (resulting from the solution of the optimization problem of the former step) N^2 randomly chosen local transformations $\exp\{i \sum_{i \in \text{local}} \alpha_i \widehat{g}_i^N\}$, generating $\sim N^4$ new product states. New entangled states can be generated by applying random generic transformations $\exp\{i \sum_{i=1}^{N^2-1} \beta_i \widehat{g}_i^N\}$ to each of the entangled states obtained in the previous step, where i numerates the generators of the $SU(N)$ group while $i \in \text{local}$ the generators of the subgroup of local transformation. Random parameters are normally distributed with width gradually decreasing as the number of the iteration steps decreases. The linear programming problem is solved again for $\sim N^4$ vertices in these two new polytopes and iteratively repeats until the result converges. Note that for each subsequent step, the presence of the solution of the former step of the loop is essential in order to guarantee an outcome from the linear programming algorithm. The set of the eigenvectors of the density matrix plays this role for the first step. Numerical inspection shows that the final results of the algorithm, i.e., the product component $\widehat{\rho}_{\text{sep}}$ and the essentially entangled part $\widehat{\rho}_{\text{ent}}$, Eqs. (6) and (7), are always the same for different sets of algorithm iterations.

The algorithm described above addresses the case of full separability of a state or the identification of the essentially K -entangled component. The same set of steps can be applied if we make a repartition of the initial system and consider L separability of the state with $L < K$. Furthermore, if the set of separable states is enlarged to include other special classes of pure states, e.g., states of the W class [16], then one can apply the algorithm in order to reveal the classification of mixed multipartite entangled state as the one introduced in [17] for three qubits. We would like to mention here that for the specific case of three qubits in mixed state, there has been a lot of progress concerning the classification of entanglement via analytic criteria and efficient algorithms [18–20].

IV. SUGGESTIONS FOR CHARACTERIZING ENTANGLEMENT PROPERTIES OF THE ESSENTIALLY ENTANGLED COMPONENT

One may claim that all information relevant to entanglement is contained in the essentially entangled part $\widehat{\rho}_{\text{ent}}$ of the density matrix. Though this is not the main object of this work, we make some simple suggestions for analyzing entanglement properties of $\widehat{\rho}_{\text{ent}}$ employing previous results [21] about characterization of entanglement for pure states.

For pure quantum states, entanglement is directly related to the factorability of state vectors, and therefore one can characterize entanglement by identifying the orbit of local transformations for a given state. This orbit can be marked by a complete set of polynomial invariants or alternatively, by the coefficients $\{\beta\}$ of the tanglemeter $\widehat{NI}(\{\beta\}) = \sum_{i, \dots, j} \beta_{i, \dots, j} \sigma_i^+ \dots \sigma_j^+$ of a given state [21]. The state defined as $|c(\{\beta\})\rangle = \exp[\widehat{NI}(\{\beta\})]|0\rangle$ is the so-called canonical state, and this can be reached from the state under study by the action of local operations under the constraint that the population of the reference state $|0\rangle$ is maximized. In addition to the identification of the orbit of local transformations, the tanglemeter generalizes the concept of logarithm to vectors

and its coefficients straightforwardly reveal the factorization properties of the state.

Entanglement of mixed states cannot rely only on one operation of group multiplication but also involves the procedure of casting in convex sums. Therefore the algebraic structure does not suggest a natural framework for the characterization of entanglement in this case. Construction of an approach to entanglement characterization is a convenience complementing the exhaustive information contained in the essentially entangled part of the density matrix.

A straightforward way to characterize entanglement of mixed states would be to find the tanglemeeters of the eigenstates of ρ_{ent} . It does not mean that an entangled state corresponding to another orbit cannot be detected. Any pure state which belongs to the essentially entangled subspace H_E spanned by the eigenvectors of $\hat{\rho}_{\text{ent}}$ is also a legitimate representative of the ensemble of entangled states associated with this density matrix. One therefore may want to find the ‘‘corners’’ of this ensemble of states by identifying the state $|c_1\rangle$ in H_E closest to the set of product states \mathcal{P} , followed by identification of a state $|c_2\rangle \perp |c_1\rangle$ closest to \mathcal{P} then, $|c_3\rangle \perp |c_2\rangle, |c_1\rangle$ etc., until $|c_{d_E}\rangle$, and calculate tanglemeeters for these ‘‘corners.’’ Tanglemeter coefficients of any state in H_E will therefore be within the borders given by these ‘‘corners.’’ We would like to mention here that the use of the tanglemeter as a method for characterizing multipartite entanglement is not essential. One may apply this idea to other measures of multipartite entanglement for pure states, as are the entanglement monotones from antilinear operators introduced in [22].

Another option is to find the tanglemeter coefficients distribution function,

$$P(\{\beta\}) = \int \langle c(\{\beta(x)\}) | \hat{\rho}_{\text{ent}} | c(\{\beta(x)\}) \rangle \delta(\{\beta(x) - \beta\}) d\mu_{x \in H_E}, \quad (12)$$

resulting from averaging over the Haar measure $\mu_{x \in H_E}$ in the subspace H_E in accordance with Eq. (9) of weight suggested by $\hat{\rho}_{\text{ent}}$ (the probability to have a canonic state with given tanglemeter coefficients). The number $P(\{\beta\})$ gives the probability density of finding an entangled state which belongs to the orbit characterized by the set $\{\beta\}$ of the tanglemeter coefficients. In the case where one of the eigenvalues of $\hat{\rho}_{\text{ent}}$ is much larger than others, the probability distribution $P(\{\beta\})$ is located near the tanglemeter of the corresponding eigenvector and can be adequately characterized by a small covariance matrix of the tanglemeter’s coefficients.

V. EXAMPLE

We now present an illustration of the introduced methods with a physical example of an open system experiencing loss of coherence due to the presence of classical noise. The model is comprised of three elements: two two-level systems and one three-level system. The local symmetry group is the SU(2) group for each of the two-level systems, the SU(3) group for the three-level, and the SU(12) for the total assembly the group of transformations (local and nonlocal). We consider the combined physical system of a p -state atom ($L = 1$, $M_L = -1, 0, 1$) in a static magnetic field, which parametrically

interacts with a two-mode electromagnetic field. We also assume that each of the field modes allows for two possible polarizations of the photons.

The Hamiltonian of the system consists of four parts:

(i) the Hamiltonian of the first field mode $\hat{H}_1 = k_z(\hat{a}_x^\dagger \hat{a}_x + \hat{a}_y^\dagger \hat{a}_y)$, with wave vector k_z and polarizations x and y ,

(ii) the Hamiltonian of the second mode $\hat{H}_2 = k_x(\hat{b}_y^\dagger \hat{b}_y + \hat{b}_z^\dagger \hat{b}_z)$, with wave vector k_x ,

(iii) the Hamiltonian of the atom $\hat{H}_3 = (\mathbf{H}\hat{\mathbf{L}})$ in the static magnetic $\mathbf{H} = \{H_x, H_y, H_z\}$ field, where $\hat{\mathbf{L}}$ is the angular momentum vector operator, and

(iv) the Hamiltonian describing the parametric interaction

$$\hat{H}_4 = \frac{(\hat{a}_x^\dagger \hat{a}_y + \hat{a}_y^\dagger \hat{a}_x) \hat{X} \hat{Y}}{k_z - \omega_1} + \frac{(\hat{b}_y^\dagger \hat{b}_z + \hat{b}_z^\dagger \hat{b}_y) \hat{Y} \hat{Z}}{k_x - \omega_2}, \quad (13)$$

which results from the second-order perturbation theory applied over the dipole interaction $(\hat{a}_x^\dagger + \hat{a}_x) \hat{X} + (\hat{a}_y^\dagger + \hat{a}_y) \hat{Y} + (\hat{b}_z^\dagger + \hat{b}_z) \hat{Z} + (\hat{b}_y^\dagger + \hat{b}_y) \hat{Y} + (\hat{b}_z^\dagger + \hat{b}_z) \hat{Z}$.

Here \hat{a}_i^\dagger and \hat{b}_i^\dagger are the photon creation operators of the first and the second mode, corresponding to polarization along the direction i , while \hat{a}_i and \hat{b}_i are their conjugate photon annihilation operators. ω_1 and ω_2 are the frequencies of the allowed dipole atomic transition from the state p that are closest to the respective frequencies of the first k_z and the second k_x photon modes. The atomic optical electron radius-vector operator $\hat{\mathbf{R}} = \{\hat{X}, \hat{Y}, \hat{Z}\}$ and the angular momentum vector operator $\hat{\mathbf{L}} = \{\hat{L}_x, \hat{L}_y, \hat{L}_z\}$ enter the Hamiltonian as the respective tensor product and the scalar products with the magnetic field, while the light velocity, the electron charge, and the Planck’s constant are set to unity.

Since parametric interaction implies conservation of the total number of photons of the two modes, $\hat{H}_1 + \hat{H}_2$ is an integral of motion for the system and only the Hamiltonians \hat{H}_3 and \hat{H}_4 are responsible for the dynamical process of interest. The relevant part $\hat{H} = \hat{H}_3 + \hat{H}_4$ can be rewritten in a more convenient way, noting that the x , y , and z components of the vector-operator $\hat{\mathbf{L}}$ form an su(2) subalgebra of the symmetry algebra su(3) of the atomic triplet p , while the operators $\hat{X}\hat{Y}$ and $\hat{Y}\hat{Z}$ entering \hat{H}_4 as the tensor product of the components of $\hat{\mathbf{R}}$ do not belong to this subalgebra and yield other generators of the SU(3) group. All these operators can be expressed in terms of Gell-Mann matrices $\hat{\lambda}_i$ with $i = 1, \dots, 8$. The properly normalized bilinear photon operators $\hat{a}_x^\dagger \hat{a}_y + \hat{a}_y^\dagger \hat{a}_x$, $\hat{a}_x^\dagger \hat{a}_y - \hat{a}_y^\dagger \hat{a}_x$, and $\hat{a}_x^\dagger \hat{a}_x - \hat{a}_y^\dagger \hat{a}_y$ of the first mode form an su(2) algebra, as do the similar operators of the second mode. Therefore these can be expressed in terms of the respective Pauli matrices $\hat{\sigma}_{1,i}$ and $\hat{\sigma}_{2,i}$, where $i = x, y, z$. In summary, the Hamiltonian $\hat{H} = \hat{H}_3 + \hat{H}_4$ can be cast in the form

$$\hat{H} = \sum_{i=1}^3 \hat{\lambda}_i f_i + f_4 \hat{\sigma}_{1,x} \hat{\lambda}_4 + f_6 \hat{\sigma}_{2,x} \hat{\lambda}_6 + \varepsilon_1 \hat{\sigma}_{1,z} + \varepsilon_2 \hat{\sigma}_{2,z}, \quad (14)$$

where the parameters $f_{i=1,2,3}$ depend on the static field, parameters f_4 and f_6 are governed by the detuning of the photon frequencies from the atomic transition frequencies, and parameters $\varepsilon_{i=1,2}$ deviate from zero when the photon frequency turns to be dependent on the polarization in the presence of

an anisotropy of the refraction index (that is, when k_z is slightly different for the x and y polarizations, and similarly for k_x).

Now let us consider a realistic situation where the static field experiences small and rapid fluctuations, where $f_i(t) = \bar{f}_i + \delta f_i(t)$ for $i = 1, 2, 3$. In this case the Liouville equation $i\dot{\hat{\rho}} = [\hat{H}(t), \hat{\rho}]$ describing the time evolution of the density matrix $\hat{\rho}(t)$ of the assembly can be averaged over these rapid fluctuations $\delta f_i(t)$, yielding the following Lindblad master equation [23]:

$$i\dot{\hat{\rho}} = [\overline{\hat{H}}, \hat{\rho}] - i \sum_{i,j=1}^3 \overline{\delta f_i(t)\delta f_j(t)} [\hat{\lambda}_i, [\hat{\lambda}_j, \hat{\rho}]], \quad (15)$$

where the upper bar denotes the time average. Substitution of this master equation in the Liouville representation

$$\hat{\rho}(t) = \sum_{i=0}^{143} r_i(t) \hat{g}_i^{12} \quad (16)$$

of the density matrix in terms of the generators of the unitary group $SU(12)$ yields a system of 143 linear, first-order differential equations:

$$i\dot{r}_k = \sum_{m=1}^{143} (\text{Tr}\{\hat{g}_k^{12} [\overline{\hat{H}}, \hat{g}_m^{12}]\} - i\mathcal{R}_{k,m}) r_m, \\ \mathcal{R}_{k,m} = \sum_{i,j=1}^3 \overline{\delta f_i(t)\delta f_j(t)} \text{Tr}\{\hat{g}_k^{12} [\hat{\lambda}_i, [\hat{\lambda}_j, \hat{g}_m^{12}]]\}, \quad (17)$$

for the real vector components $r_i(t)$. The straightforward analytic solution of Eq. (17) gives oscillations with time for some of the coefficients $r_i(t)$, while others die off with rates determined by the relaxation operator $\mathcal{R}_{k,m}$.

A considerable amount of work on the understanding of the dynamics of entanglement has been performed in [3]. Figure 2

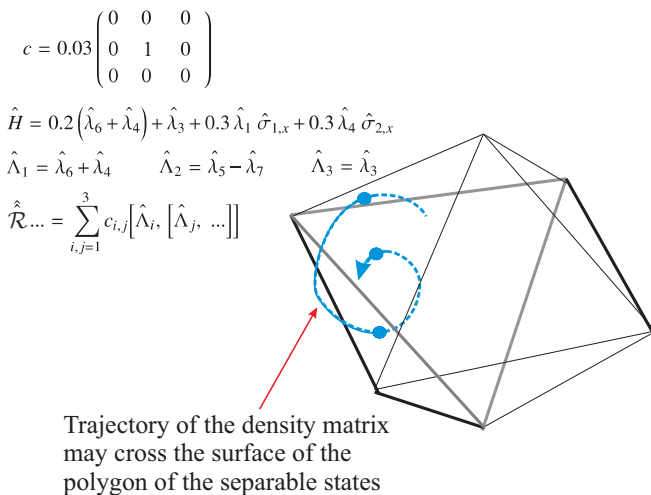


FIG. 2. (Color online) A symbolic description of the trajectory in the Liouville space of a mixed state undergoing loss of coherence due to interaction with the environment. Crossing of the polytope of the separable states results in sudden death (or birth) of entanglement. The inset lists the numerical values of the parameters of the model.

graphically represents a generic solution for this example as a spiral in the Liouville space gradually approaching a stationary solution. This picture also provides a complementary point of view on the phenomenon of sudden death and revival of entanglement [24]. During the course of time, it is expected that the essentially entangled part will oscillate between different subspaces and eventually vanish for periods of time when the density matrix is passing inside the polytope of separable states (Fig. 2). The revival of entanglement is marked by the exit of the density matrix from the polytope. This graphical representation can be justified by the calculations as follows.

We now solve the model Eq. (17) for a set of given values for f_i presented in Fig. 2 and reconstruct the density matrix $\hat{\rho}(t)$ with the help of Eq. (16), where Fig. 3 summarizes the calculation results. Figure 3(a) graphs the purity $P(t) = \text{Tr}[\hat{\rho}^2(t)]$ of the density matrix as a function of time. At each time step the algorithm is applied and the density matrix is decomposed as $\hat{\rho}(t) = [1 - B(t)]\hat{\rho}_{\text{sep}}(t) + B(t)\hat{\rho}_{\text{ent}}(t)$, Eq. (2). Figure 3(b) graphs the weight $B(t) = \sum_{i=1}^m b_i$, Eq. (5), of the essentially entangled component in the density matrix. The weight $B(t)$ is decreasing with time faster than the purity does, and it exhibits some oscillatory behavior that can be possibly explained by motion of the essentially entangled component along the facets of the polytope. Figure 3(c) plots the rank d_E of $\hat{\rho}_{\text{ent}}(t)$, and this moves in a rather random fashion between the values of 1 and 5. If full ($K = 3$) separability is considered, then $d_{E \text{ max}} = 7$. In our program we have included in the “polytope” of separable states the biseparable states; therefore $d_{E \text{ max}} = 5$. The “jumps” of the rank demonstrate the recursive move of an essentially entangled component between different essentially entangled subspaces on S_{CH} . Moreover, in the time interval [18.8–19.7], $B(t)$ vanishes, implying that the state enters inside the polytope of separable states. This physical situation describes a sudden death and sudden revival of entanglement, a phenomenon [24–26] which has been studied extensively with other methods. Our geometric decomposition offers additional information on the origin of this phenomenon, as shown in Fig. 2.

In order to analyze the entanglement properties of the essentially entangled component, we first note that for the chosen model system, in the vast majority of the time steps there is a dominant eigenvector \hat{e}_{dom} for $\hat{\rho}_{\text{ent}}$ with a corresponding eigenvalue $\lambda_{\text{dom}} > 0.9$ [Fig. 3(d)]. Therefore, for this specific example and assigned parameters, it is possible to analyze just the entanglement properties of \hat{e}_{dom} , whenever the condition $\lambda_{\text{dom}} > 0.9$ is satisfied, and to conclude from this analysis the entanglement properties of $\hat{\rho}_{\text{ent}}$. Naturally, this analysis, together with the weight $B(t)$, results in all the information necessary to describe entanglement in $\hat{\rho}$.

We analyze the entanglement properties of \hat{e}_{dom} with the help of the method of nilpotent polynomials [21]. In the Appendix we provide an explicit method for deriving the general expression for the tanglemeter of a wave vector describing an assembly of a three-level system and two two-level systems:

$$\widehat{Nl}(\{\beta\}) = (\beta_{110}\hat{t}^+\hat{\sigma}_1^+ + \beta_{101}\hat{t}^+\hat{\sigma}_2^+ + \beta_{011}\hat{\sigma}_1^+\hat{\sigma}_2^+ \\ + \beta_{210}\hat{u}^+\hat{\sigma}_1^+ + \beta_{201}\hat{u}^+\hat{\sigma}_2^+ \\ + \beta_{111}\hat{t}^+\hat{\sigma}_1^+\hat{\sigma}_2^+), \quad (18)$$

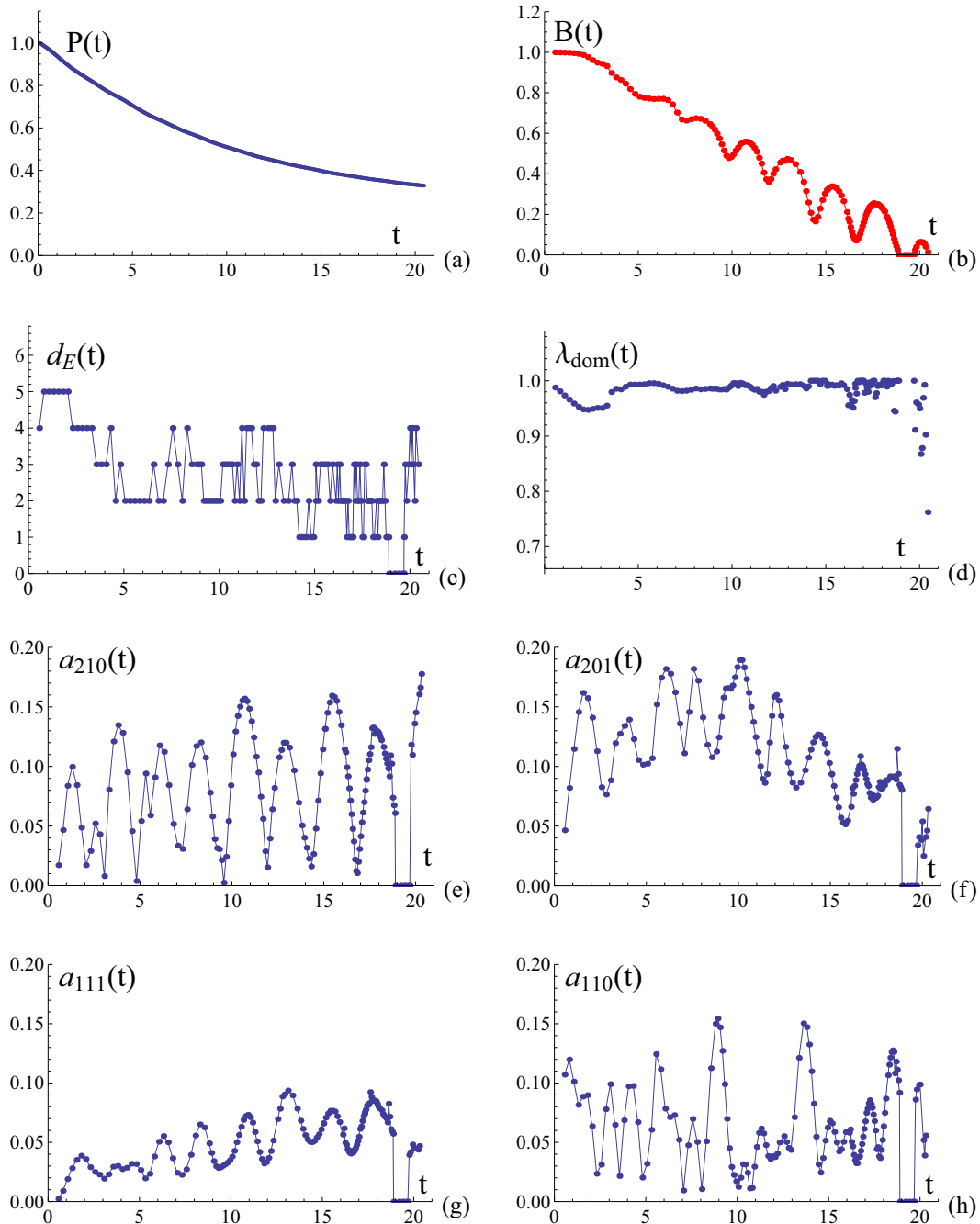


FIG. 3. (Color online) We solve the Lindblad equation for the example and we apply the algorithm at each time step: (a) purity of the assembly, (b) the statistical contribution of $\hat{\rho}_{\text{ent}}(t)$ to the density matrix, (c) the rank of $\hat{\rho}_{\text{ent}}(t)$, (d) the eigenvalue of the dominant eigenvector of $\hat{\rho}_{\text{ent}}(t)$, and (e–h) the oscillations of the real coefficients of the tanglemeter. In the time interval [18.8–19.7], sudden death of entanglement takes place and then its revival.

with $\beta_{111}, \beta_{201}, \beta_{210}, \beta_{110}$ being positive numbers and β_{101}, β_{011} being complex. The matrix representation of the nilpotent variables (operators) $\hat{u}^+, \hat{v}^+, \hat{\sigma}^+$ is also provided in the Appendix. The coefficients of the tanglemeter are not entanglement monotones [2] in the strict sense; these are invariant under the action of local transformations, and the presence of any nonzero term in the tanglemeter ensures the presence of entanglement. More precisely, the coefficient β_{111} ensures the presence of genuine tripartite entanglement in the state while the rest of the coefficients are related to the bipartite

entanglement. Figures 3(e)–3(h) plot those coefficients which are positive, and these coefficients oscillate without dissipation through time. The same holds for the real and imaginary parts of the complex coefficients not shown in the figure.

With this example, in addition to the death and revival of entanglement, we observe two interesting phenomena which need more study in order to determine whether they are specific to this example or more general. The first is the presence of a dominant eigenvector in the essential entangled component, and the second is the oscillations

without dissipation of the entanglement characteristics of the essential entangled component.

VI. CONCLUSIONS

In this work we have introduced the concept of the essentially entangled component of a mixed multipartite state, analyzed its properties, and suggested an algorithm for its numerical identification. This concept is closely related to the best separable approximation introduced in [13], but in this current work we have developed and exploited the geometric aspects of it. More specifically, we have introduced and analyzed the properties of the essentially entangled component employing the geometric description of mixed quantum states that result from the decomposition of a density matrix over the generators of the relevant group. Furthermore, we have exploited this generalized Bloch sphere picture to construct an efficient linear programming algorithm for finding the essentially entangled component of a given state. This algorithm not only gives a numerical answer to the separability problem, but also identifies the vector component of the density matrix relevant to entanglement. Finally, we introduced a specific example to study the entanglement dynamics of an open quantum system by reconstructing the time trajectory of the essentially entangled component of the system. Sudden death and sudden birth of entanglement can be clearly understood in the introduced geometric picture, while other interesting new aspects of entanglement in open quantum systems are observed.

The algorithm introduced in this work scales polynomially with the dimension of the system in the general case [5] and it can be used to study open questions about entanglement in mixed states. For example, this algorithm can be straightforwardly applied to address the question of the relative volume of separable states over entangled mixed states as a function of the total purity of the system and the total dimension of the system [27]. The answer to this example can serve as an evaluation method for emerging quantum technologies and their quantum limits. Finally, the essentially entangled component containing all entanglement properties of the density matrix may also provide new directions to entanglement detection [28] and entanglement distillation [29] techniques.

ACKNOWLEDGMENTS

V.A. acknowledges stimulating and useful discussions with Mikhail Tsvasman and Sergey Pirogov and the hospitality accorded to him at Laboratoire J.-V. Poncelet CNRS. V.A. and A.M. are thankful to Jens Siewert for indicating to them important related works. A.M. acknowledges financial support from the Ministry of Education and Science of the Republic of Kazakhstan (Contract No. 339/76-2015).

APPENDIX

1. A second formulation and proof of the main theorem

Here we provide a more detailed formulation and proof for the theorem given in Sec. II, which does not rely on a particular quantum-mechanical representation.

The maximum rank $d_{E\max}$ of an essentially entangled component is $N_{CG} - N_{CS}$, where N_{CG} is the dimension of the Cartan subgroup of the group of all transformations on the state and N_{CS} is the dimension of Cartan (sub)subgroup generating only local transformations.

Remark. The numbers N_{CG} and N_{CS} give the respective numbers of complex parameters characterizing generic and product state vectors on $N = N_{CG} + 1$ dimensional Hilbert spaces.

Proof. Consider a density matrix $\hat{\rho}$ and its decomposition to the essentially entangled and separable part $\hat{\rho} = (1 - B)\hat{\rho}_{\text{sep}} + B\hat{\rho}_{\text{ent}}$. Since B corresponds to a minimum value of all possible weights, we conclude that no $\epsilon > 0$ and product vector $|p\rangle$ exist such that $\hat{\rho}_{\text{ent}} - \epsilon|p\rangle\langle p|$ is a positive matrix. Considering the essentially entangled subspace H_E spanned by the eigenvectors $|\psi_i\rangle$ with nonzero eigenvalues of $\hat{\rho}_{\text{ent}}$ with $i = 1, \dots, d_E$, this condition means that no product state $|p\rangle$ exists in H_E . For the case where

$$|p\rangle = \sum_{i=1}^{d_E} |\psi_i\rangle + \epsilon'|p'\rangle, \quad (\text{A1})$$

with $\langle p'|\psi_i\rangle = 0$ for every $i = 1, \dots, d_E$, one identifies the vector $|p'\rangle$ orthogonal to the subspace of d_E eigenvectors, which makes

$$\langle p' | (\hat{\rho}_{\text{ent}} - \epsilon|p\rangle\langle p|) | p'\rangle = -\epsilon |\langle p|p'\rangle|^2 < 0, \quad (\text{A2})$$

and therefore extremality implies that no product state is orthogonal to the orthogonal complement H_E^\perp of H_E spanned by the eigenvectors $|\psi_i\rangle$ of $\hat{\rho}_{\text{ent}}$ with zero eigenvalues and $i = d_E, \dots, N_{CG}$.

In other words, in order to find such a state we have to satisfy $N_{CG} - d_E$ equations $\langle p|\psi_i\rangle = 0$ with $i = d_E + 1, \dots, N_{CG}$ for a product state $|p\rangle$ given by specification of its N_{CS} parameters. This is impossible when $N_{CG} - d_E \geq N_{CS}$, which determines the maximum rank $d_{E\max}$ of $\hat{\rho}_{\text{ent}}$.

2. Deriving the tanglemeter of the physical example in Sec. V

The system under consideration consists of the two modes of the field interacting with a three-level atom. The Hilbert space is consequently of dimension $N = 12$, a direct product of the spaces of two two-level systems (qubits) and of one three-level system (qutrit). In the standard computational basis, a state vector of the system is expressed as

$$\begin{aligned} |\Psi\rangle = & \psi_{000}|000\rangle + \psi_{100}|100\rangle + \psi_{200}|200\rangle + \psi_{010}|010\rangle \\ & + \psi_{001}|001\rangle\psi_{110}|110\rangle + \psi_{101}|101\rangle + \psi_{011}|011\rangle \\ & + \psi_{210}|210\rangle + \psi_{201}|201\rangle + \psi_{111}|111\rangle + \psi_{211}|211\rangle, \end{aligned}$$

or alternatively, using the nilpotent creation operators

$$\hat{u}^+ = \begin{pmatrix} 0 & 0 & 1 \\ 0 & 0 & 0 \\ 0 & 0 & 0 \end{pmatrix}, \quad (\text{A3})$$

$$\hat{t}^+ = \begin{pmatrix} 0 & 0 & 0 \\ 0 & 0 & 1 \\ 0 & 0 & 0 \end{pmatrix}, \quad (\text{A4})$$

$$\hat{\sigma}^+ = \begin{pmatrix} 0 & 1 \\ 0 & 0 \end{pmatrix}, \quad (\text{A5})$$

as

$$|\Psi\rangle = (\psi_{000} + \psi_{100}\hat{t}^+ + \psi_{200}\hat{u}^+ + \psi_{010}\hat{\sigma}_1^+ + \psi_{001}\hat{\sigma}_2^+ + \psi_{110}\hat{t}^+\hat{\sigma}_1^+ + \psi_{101}\hat{t}^+\hat{\sigma}_2^+ + \psi_{011}\hat{\sigma}_1^+\hat{\sigma}_2^+ + \psi_{210}\hat{u}^+\hat{\sigma}_1^+ + \psi_{201}\hat{u}^+\hat{\sigma}_2^+ + \psi_{111}\hat{t}^+\hat{\sigma}_1^+\hat{\sigma}_2^+ + \psi_{211}\hat{u}^+\hat{\sigma}_1^+\hat{\sigma}_2^+)|000\rangle.$$

The next step is the application of all the available local transformations $[\text{SU}(3) \otimes 1 \otimes 1, 1 \otimes \text{SU}(2) \otimes 1, 1 \otimes 1 \otimes \text{SU}(2)]$ on the given state $|\Psi\rangle$ in order to construct the corresponding canonic state $|\Psi_c\rangle$ which marks the orbit of local transformations. To simplify the procedure, we apply the local transformations on a given $|\Psi\rangle$ in the following order:

(a) We first apply local operations generated by the operators $\{\hat{\sigma}_1^x, \hat{\sigma}_1^y, \hat{\sigma}_2^x, \hat{\sigma}_2^y, \hat{\lambda}_4, \hat{\lambda}_5, \hat{\lambda}_6, \hat{\lambda}_7\}$ and we require that the population of the reference level $|000\rangle$ is at maximum. Under this condition the populations of the levels $|100\rangle, |200\rangle, |010\rangle, |001\rangle$ vanish.

(b) We then apply local operations generated by $\{\hat{\lambda}_1, \hat{\lambda}_2\}$ to also maximize the population of the level $|111\rangle$. The contribution of the level $|211\rangle$ also vanishes.

(c) Finally, we apply local operations generated by $\{\hat{\sigma}_1^z, \hat{\sigma}_2^z, \hat{\lambda}_3, \hat{\lambda}_8\}$ in order to make the phase of

$|111\rangle, |210\rangle, |201\rangle, |110\rangle$ equal to the phase of the amplitude of the reference level $|000\rangle$.

After this procedure one obtains the following form for the normalized canonic state:

$$|\Psi_c\rangle = (1 + \alpha_{110}\hat{t}^+\hat{\sigma}_1^+ + \alpha_{101}\hat{t}^+\hat{\sigma}_2^+ + \alpha_{011}\hat{\sigma}_1^+\hat{\sigma}_2^+ + \alpha_{210}\hat{u}^+\hat{\sigma}_1^+ + \alpha_{201}\hat{u}^+\hat{\sigma}_2^+ + \alpha_{111}\hat{t}^+\hat{\sigma}_1^+\hat{\sigma}_2^+)|000\rangle, \quad (\text{A6})$$

with $\alpha_{111}, \alpha_{201}, \alpha_{210}, \alpha_{110}$ being positive numbers and $\alpha_{101}, \alpha_{011}$ being complex.

The final step for calculating the tanglemeter $\widehat{Nl}(\{\beta\})$ of the state is to take the logarithm of the polynomial on the nilpotent variables $\hat{t}^+, \hat{\sigma}_{1,2}^+$ in Eq. (A6). In conclusion, it is easy to show that

$$\widehat{Nl}(\{\beta\}) = \beta_{110}\hat{t}^+\hat{\sigma}_1^+ + \beta_{101}\hat{t}^+\hat{\sigma}_2^+ + \beta_{011}\hat{\sigma}_1^+\hat{\sigma}_2^+ + \beta_{210}\hat{u}^+\hat{\sigma}_1^+ + \beta_{201}\hat{u}^+\hat{\sigma}_2^+ + \beta_{111}\hat{t}^+\hat{\sigma}_1^+\hat{\sigma}_2^+.$$

with $\beta_{110} = \alpha_{110}, \beta_{101} = \alpha_{101}$, etc.

-
- [1] L. Amico, R. Fazio, A. Osterloh, and V. Vedral, *Rev. Mod. Phys.* **80**, 517 (2008).
- [2] R. Horodecki, P. Horodecki, M. Horodecki, and K. Horodecki, *Rev. Mod. Phys.* **81**, 865 (2009).
- [3] L. Aolita, F. de Melo, and L. Davidovich, *Rep. Prog. Phys.* **78**, 042001 (2015).
- [4] L. Gurvits, in *Proceedings of the Thirty-Fifth Annual ACM Symposium on Theory of Computing, STOC '03* (ACM Press, New York, 2003), pp. 10–19.
- [5] In the aforesaid paper by Gurvits, it has been shown that the decision problem (whether or not a mixed state is separable) becomes NP hard in a small vicinity of the separability separatrix (the surface of the “polytope” in terms of this paper), which scales inverse exponentially with the dimensionality of the space. Later on, Gharibian, in his paper *Strong NP-hardness of the quantum separability problem* [S. Gharibian, *Quant. Inf. Comp.* **10**, 343 (2010)], showed that the situation is yet worse, since this vicinity size scales inverse polynomially with the dimension. In our opinion, such a hardness does not result from the complexity of the search algorithm but has a pure geometrical reason, simply reflecting the fact that in a multidimensional space, the accuracy of an approximation of a generic convex surface by a polytope of a given rib length scales exponentially with the space dimension. Still, for a physical problem under study of dimension N the size of aforesaid vicinity (according Gharibian’s results) remains much smaller (N^{-32}) than any reasonable physical accuracy, thus leaving the NP hardness beyond the physical interest.
- [6] A. C. Doherty, P. A. Parrilo, and F. M. Spedalieri, *Phys. Rev. Lett.* **88**, 187904 (2002).
- [7] H. J. Woerdeman, *Phys. Rev. A* **67**, 010303(R) (2003).
- [8] L. M. Ioannou, B. C. Travaglione, D. C. Cheung, and A. K. Ekert, *Phys. Rev. A* **70**, 060303(R) (2004).
- [9] F. Hulpke and D. Bru, *J. Phys. A: Math. Gen.* **38**, 5573 (2005).
- [10] F. M. Spedalieri, *Phys. Rev. A* **76**, 032318 (2007).
- [11] L. M. Ioannou, *Quant. Inf. Comp.* **7**, 335 (2007).
- [12] A. Peres, *Phys. Rev. Lett.* **77**, 1413 (1996); M. Horodecki, P. Horodecki, and R. Horodecki, *Phys. Lett. A* **223**, 1 (1996).
- [13] M. Lewenstein and A. Sanpera, *Phys. Rev. Lett.* **80**, 2261 (1998).
- [14] C. M. Caves and G. J. Milburn, *Opt. Commun.* **179**, 439 (2000).
- [15] M. S. Byrd and N. Khaneja, *Phys. Rev. A* **68**, 062322 (2003); G. Kimura, *Phys. Lett. A* **314**, 339 (2003).
- [16] W. Dür, G. Vidal, and J. I. Cirac, *Phys. Rev. A* **62**, 062314 (2000).
- [17] A. Acin, D. Bruss, M. Lewenstein, and A. Sanpera, *Phys. Rev. Lett.* **87**, 040401 (2001).
- [18] R. Lohmayer, A. Osterloh, J. Siewert, and A. Uhlmann, *Phys. Rev. Lett.* **97**, 260502 (2006).
- [19] B. Jungnitsch, T. Moroder, and O. Gühne, *Phys. Rev. Lett.* **106**, 190502 (2011).
- [20] S. Rodrigues, N. Datta, and P. Love, *Phys. Rev. A* **90**, 012340 (2014).
- [21] A. Mandilara, V. M. Akulin, A. V. Smilga, and L. Viola, *Phys. Rev. A* **74**, 022331 (2006).
- [22] A. Osterloh and J. Siewert, *Phys. Rev. A* **72**, 012337 (2005).
- [23] V. M. Akulin, *Dynamics of Complex Quantum Systems* (Springer, New York, 2014), pp. 228–231.
- [24] T. Yu and J. H. Eberly, *Phys. Rev. Lett.* **93**, 140404 (2004); J. H. Eberly and T. Yu, *Science* **316**, 555 (2007).
- [25] B. V. Fine, F. Mintert, and A. Buchleitner, *Phys. Rev. B* **71**, 153105 (2005).
- [26] C. E. Lopez, G. Romero, F. Lastra, E. Solano, and J. C. Retamal, *Phys. Rev. Lett.* **101**, 080503 (2008).
- [27] K. Zyczkowski, P. Horodecki, A. Sanpera, and M. Lewenstein, *Phys. Rev. A* **58**, 883 (1998).
- [28] Gühne and G. Tóth, *Phys. Rep.* **474**, 1 (2009).
- [29] C. H. Bennett, G. Brassard, S. Popescu, B. Schumacher, J. A. Smolin, and W. K. Wootters, *Phys. Rev. Lett.* **76**, 722 (1996).